# Modelling of Crack Path Evolution in Round Bars under Cyclic Tension and Bending

**J. Toribio[1], J. C. Matos[2], B. González[1] and J. Escuadra[2]**

[1] Department of Materials Engineering - University of Salamanca - E.P.S. Zamora (Spain). toribio@usal.es
[2] Department of Computing Engineering - University of Salamanca - E.P.S. Zamora (Spain). jcmatos@usal.es

***ABSTRACT.*** *This paper shows the evolution of the surface crack front in round bars constituted of different materials (determined by the exponent m of the Paris law), subjected to fatigue tension loading (with free ends) or fatigue bending loading. To this end, a numerical modeling was developed on the basis of a discretization of the crack front (characterized as an ellipse) and the crack advance at each point perpendicular to such a front, according to a Paris-Erdogan law, using a three-parameter stress intensity factor (SIF). Each analyzed case was characterized by the evolution of the semielliptical crack front, studying the progress with the relative crack depth a/D of the following three key variables: (i) crack aspect ratio a/b (relation between the semiaxes of the ellipse which defines the crack front); (ii) maximum dimensionless SIF; (iii) minimum dimensionless SIF.*

## INTRODUCTION

One of the most relevant geometries in the field of fatigue and fracture mechanics applied to the structural engineering is a cracked cylinder under tension loading or bending moment. As a matter of fact, many structural elements, mainly in civil engineering consist of wires, bolts, shafts, cables or other components of cylinder shapes under constant or cyclic loading, so that the risk of surface cracking by mechanical or environmental actions is not negligible.

Growth of surface cracks in round bars due to fatigue can be modeled using different criteria. Prediction of the 90º intersecting angle of the crack with the surface or the iso-$K$ criterion along the crack front exhibit small differences in their aspect ratio but both lead to a unique fitting [1]. Another criterion is based on the crack growth according to the Paris Erdogan law considering the crack advance perpendicular to the crack front, assuming elliptic geometry of the crack [2-4], avoiding the shape hypothesis [5,6] or using the modified Forman model [7].

Characterization of fatigue crack growth, whose crack front has been commonly represented as straight, circular or elliptical with centre on the wire surface, necessarily implies knowing the dimensionless stress intensity factor (SIF), $Y$, which makes it

essential to discern how it changes along the crack front. The dimensionless SIF has been obtained by several authors under different loading conditions (tension, bending and torsion) and deducted from different procedures: flexibility method, finite element method, contour integral analysis, experimental techniques, etc. [2-3,8-12].

Fatigue crack growth in round bars with different initial geometry leads to a preferential crack path, with an aspect ratio between 0.6 and 0.7 for a relative crack depth close to 0.6 for tension [2,5], since the geometry of the crack front must be defined with, at least, two independent parameters [9]. Growth patterns are closer for a higher value of the Paris coefficient m. The crack always tries to propagate towards an iso-*K* configuration; however, it can not be maintained due to the existence of the surface, where the stress has a two-dimensional state and the singularity of the square root can be lost at the crack tip [5].

## NUMERICAL MODELLING

In order to study how a crack propagates on the cross section of a round bar under tension or bending cyclic loading (Fig. 1), a computer program in Java programming language was developed to determine the geometrical evolution of the crack front.

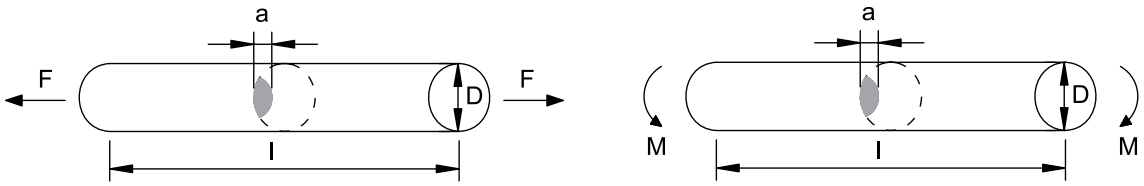


Figure 1. Cracked bar under tension loading (left) and bending moment (right).

The basic hypothesis of the modeling consisted of assuming that the crack front can be modeled as an ellipse with centre on the bar surface [13] and the fatigue propagation takes place in a direction perpendicular to this crack front, following a Paris Erdogan law [14],

$$\frac{\mathrm{d}a}{\mathrm{d}N} = C\Delta K^{\mathrm{m}} \tag{1}$$

Every elliptical arc of the crack was divided in *z* segments with exactly the same length using the Simpson method to discretize the front. The point on the wire edge was not taken into account, since it presents some difficulties regarding the computation of the dimensionless SIF (there is a plane stress state on the crack edge). After that, every single point was shifted according to Paris Erdogan law perpendicular to the front, so as to keep constant the maximum crack depth increment, $\Delta a(\max) \equiv \max \Delta a_{\mathrm{i}}$. The advance of every front point, $\Delta a_{\mathrm{i}}$, can be obtained from the maximum crack increment and the ratio of the dimensionless SIF,

$$\Delta a_{\mathrm{i}} = \Delta a(\max)\left[\frac{Y_{\mathrm{i}}}{Y(\max)}\right]^{\mathrm{m}} \tag{2}$$

The newly obtained points, fitted by the least squares method [13], generate a new ellipse with which the process is repeated iteratively until the desired crack depth is reached. Due to the existing symmetry, only half of the problem was used for the computations (Fig. 2).

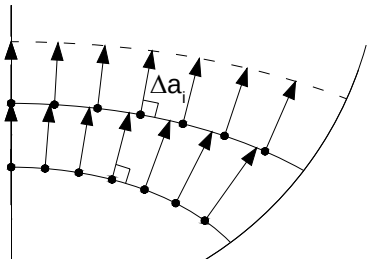


Figure 2. Process followed to compute the fatigue crack growth.

The dimensionless SIF used in the computations is that proposed by Shin and Cai [4] obtained by the finite element method together with a virtual crack extension technique, which depends on the crack geometry $a/b$, the crack depth $a/D$ and the position of the point considered on its front $x/h$ (Fig. 3).

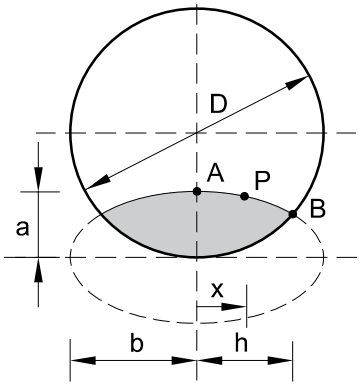


Figure 3. Elliptical crack model used by Shin and Cai.

The fitting of the results provides three-parametrical expressions which are defined as a function of the coefficients $M_{ijk}$ for tension with free ends [4],

$$Y = \sum_{i=0}^{2}\sum_{j=0}^{7}\sum_{k=0}^{2} M_{ijk}\left(\frac{a}{b}\right)^{i}\left(\frac{a}{D}\right)^{j}\left(\frac{x}{h}\right)^{k} \tag{3}$$

and of coefficients $N_{ijk}$ for bending [4].

$$Y = \sum_{i=0}^{2}\sum_{j=0}^{6}\sum_{k=0}^{2} N_{ijk}\left(\frac{a}{b}\right)^{i}\left(\frac{a}{D}\right)^{j}\left(\frac{x}{h}\right)^{k} \tag{4}$$

## NUMERICAL RESULTS AND DISCUSSION

The study of the convergence was performed to obtain the number of segments in which each ellipse is divided, $z$, and the value of the maximum crack increase, $\Delta a(\max)$ [15]. The geometrical evolution of the crack front, characterized as part of the ellipse, was determined for every relative crack depth, $a/D$, through the aspect ratio, $a/b$ (Figs. 4 to 6). These figures plot the evolution of the aspect ratio a/b with crack growth (represented by the relative crack depth $a/D$) for materials with Paris exponent $m$=2, 3 and 4.

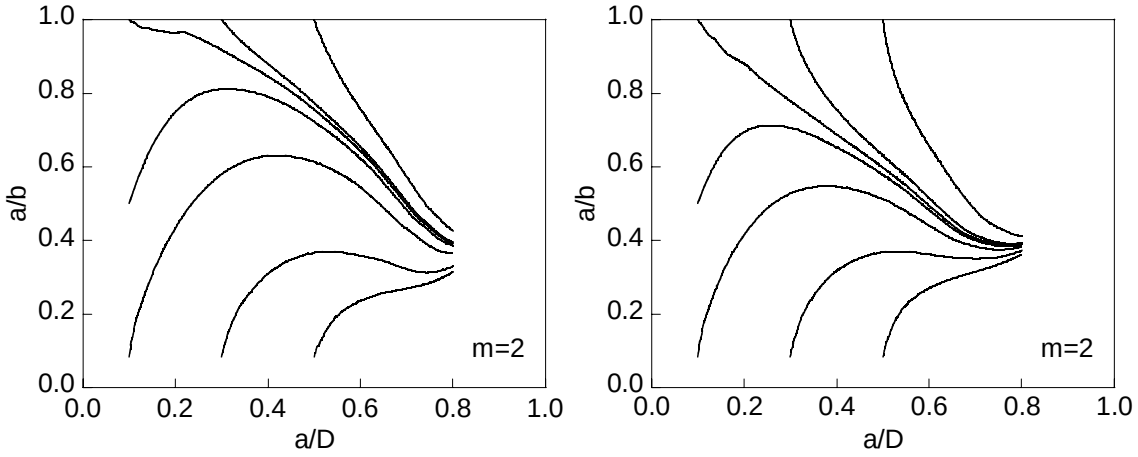


Figure 4. Evolution of the aspect ratio $a/b$ with crack growth (represented by the relative crack depth $a/D$) for a material with Paris exponent $m$=2, starting from different initial crack geometries (corresponding to the beginning of each curve, i.e., the point of minimum crack depth $a/D$) under tension loading (left) and bending moment (right).

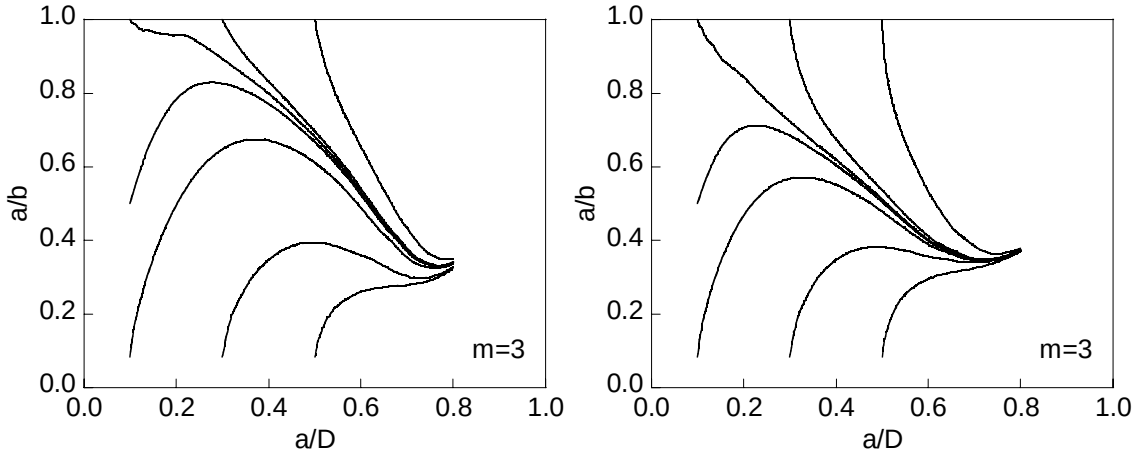


Figure 5. Evolution of the aspect ratio $a/b$ with crack growth (represented by the relative crack depth $a/D$) for a material with Paris exponent $m$=3, starting from different initial crack geometries (corresponding to the beginning of each curve, i.e., the point of minimum crack depth $a/D$) under tension loading (left) and bending moment (right).

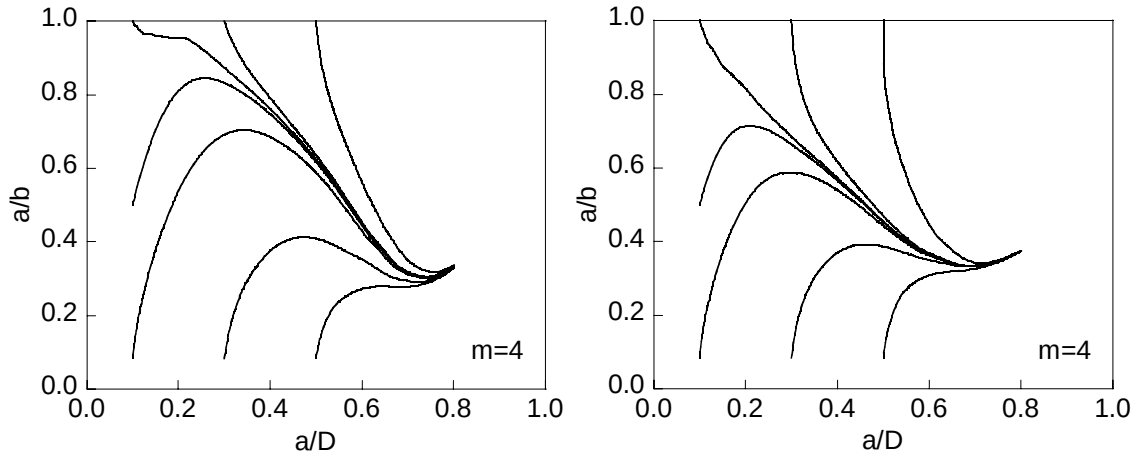


Figure 6. Evolution of the aspect ratio $a/b$ with crack growth (represented by the relative crack depth $a/D$) for a material with Paris exponent $m$=4, starting from different initial crack geometries (corresponding to the beginning of each curve, i.e., the point of minimum crack depth $a/D$) under tension loading (left) and bending moment (right).

Under fatigue loading, different initial crack configurations tend to a preferential path (in a plot $a/b$-$a/D$), the convergence (proximity between the curves representing the crack advance from different initial crack shapes) being faster for higher values of the $m$-coefficient of the Paris law and greater for the bending loading than for the tensile loading. It is observed that results depend on the exponent of the Paris law (Paris coefficients), so that for $m$=2 and $m$=3 fronts are more distant between them than for $m$=3 and $m$=4, where the $m$=3 front is between $m$=2 and $m$=4.

When subjected to bending, growth curves generally present lower values for the $a/b$ parameter than under tension, with the exception of the deepest cracks growing from an initial crack aspect ratio $(a/b)_0 \cong 0$. If the initial crack is circular (i.e., $(a/b)_0=1$), the aspect ratio a/b diminishes with the crack growth, whereas when the initial crack is quasi-straight (i.e., $(a/b)_0 \cong 0$), the aspect ratio $a/b$ increases at the beginning and decreases later (with the exception of initially deep cracks with $(a/D)_0 \cong 0.5$, where the aspect ratio $a/b$ always increases), cf. Figs. 4 to 6. With quasi-circular initial geometries the aspect ratio acquires a smaller value for higher values of $m$, whereas for quasi-straight geometries it tends to higher values until crack depths close to half the diameter of the round bar, after which this tendency reverses (again with the exception of initially deep cracks with $(a/D)_0 \cong 0.5$). In addition, for $m$=3 and $m$=4 all cracks in the last stage of growth (with relative crack depth close to $a/D$=0.8) exhibit an increasing aspect ratio $a/b$.

In Fig. 7, the data obtained in this modelling are compared with those obtained by other researchers [2,4,5], for $m$=3, fatigue tensile loading with free ends and fatigue bending loading, and different initial geometries. The basis of the calculation followed by all these researchers is the same used in this paper, i.e., Paris Erdogan law [14]. Carpinteri [2] performed an advance in only two front points, the centre and one close to the round bar surface; while Lin and Smith [5] developed their

computation of the dimensionless SIF remeshing every crack advance and adjusting afterwards the fronts obtained to circles and ellipses. Shin and Cai [4] did not specify the divisions done on the crack front; however, they showed the use of a $\Delta a$(max) value of $D$/400. Generally, it can be observed that the results of the present paper agree with those of the other researchers until to a value of $a/D$=0.4. With Shin and Cai, there is an almost complete agreement, which seems reasonable because the modelling done uses the dimensionless SIF expressions computed by them. The difference with the results obtained by Carpinteri can be explained due to the variations on their dimensionless SIF values compared to those of Shin and Cai, or due to the fact that Carpinteri only used two points (the crack centre and one close to the surface bar) in the modelling.

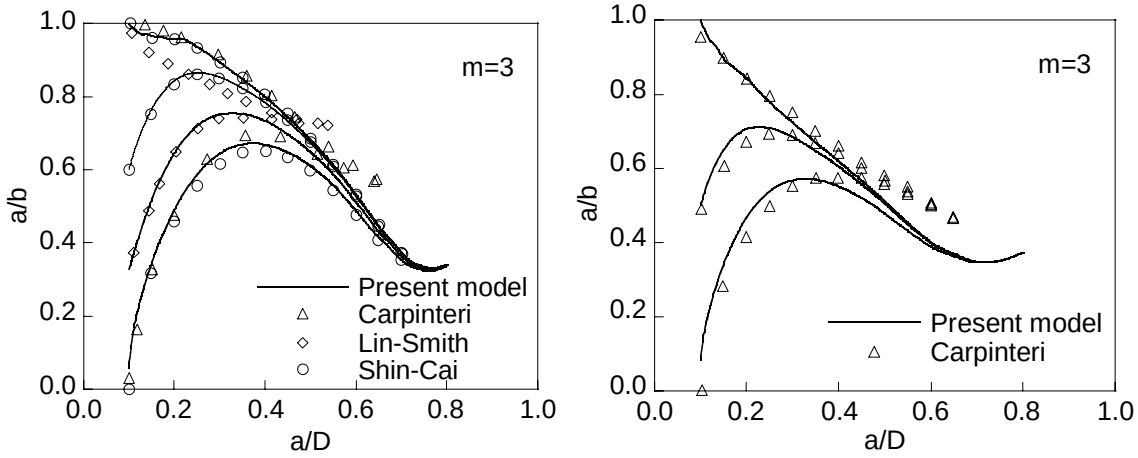


Figure 7. Comparison between predictions present model and results from other researchers: tension loading (left) and bending loading (right).

Generally, the value of the dimensionless SIF increases when so does the relative crack depth for the considered conditions in the research, converging for the different geometries of the initial crack (Figs. 8 to 10). For bending loading, the dimensionless SIF has a smaller value compared to the bar specimen subjected to tensile loading (even from smaller relative crack depths), where the dimensionless SIF under bending is roughly one third of that under tension for a relative crack depth of 0.8. Thus the risk of catastrophic failure is higher in the case of tensile loading (in relation to the less dangerous bending situation) if a local fracture criterion (on the basis of the maximum local SIF $K$ along the crack front) is used, considering that fracture takes place when $K$ reaches the material fracture toughness $K_C$.

Maximum values of the dimensionless SIF $Y_{max}$ (Figs. 8 to 10, left) also show a greater convergence than minimum values of the dimensionless SIF $Y_{min}$ (Figs. 8 to 10, right). This fact is more noticeable in bending loading (where the minimum also converges well) than in tension loading. The greater the characteristic $m$ parameter of the material, the better the convergence of the results for the different initial geometries, both of the maximum and the minimum SIF, along the crack front.

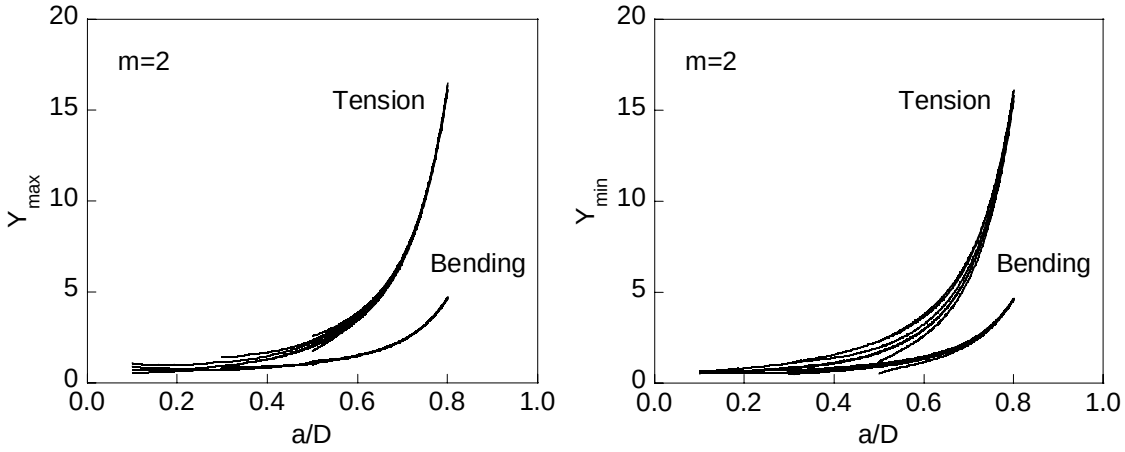


Figure 8. For *m*=2 evolution of maximum dimensionless SIF (left) and minimum dimensionless SIF (right).

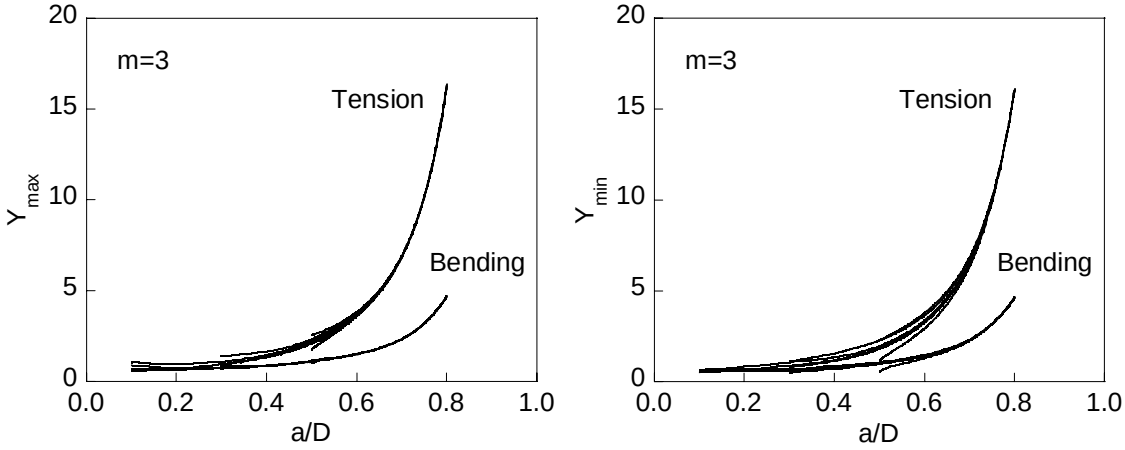


Figure 9. For *m*=3 evolution of maximum dimensionless SIF (left) and minimum dimensionless SIF (right).

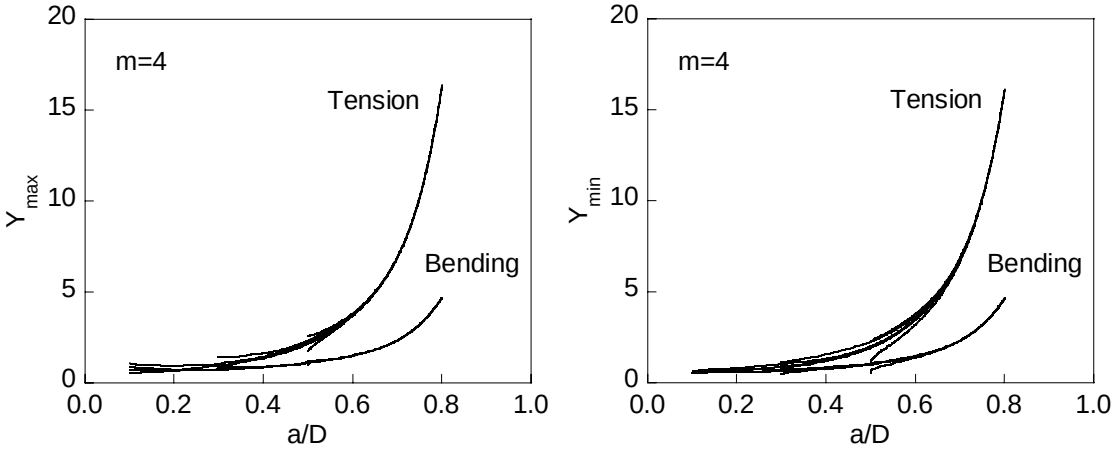


Figure 10. For *m*=4 evolution of maximum dimensionless SIF (left) and minimum dimensionless SIF (right).

## CONCLUSIONS

According to the Paris Erdogan law, in fatigue propagation the different initial crack geometries tend to a unique path on the *a*/*b vs. a*/*D* plot, this convergence (proximity between the curves representing the crack advance from different initial crack shapes) being faster for higher coefficients *m* of Paris. With quasi-circular initial geometries, the aspect ratio acquires a smaller value for higher values of *m*, whereas for quasi-straight geometries it tends to higher values until crack depths close to half the diameter of the round bar, after which this tendency reverses (with the exception of initially deep crack with $(a/D)_0 \cong 0.5$).

Maximum and minimum dimensionless stress intensity factor SIF along the crack front are smaller under bending than under tension, while the convergence of such a SIF is better under bending than under tension. Maximum dimensionless SIF presents lower dispersion than the minimum for the different initial cracks. Therefore, fracture risk due to a local fracture criterion (when the SIF value reaches fracture toughness) is higher under tension than under bending.

The greater the *m* coefficient of the Paris law, the greater the convergence of the different initial crack conditions in almost all the results: geometry of the crack front (*a*/*b*) and dimensionless SIF ($Y_{max}$, $Y_{min}$). The difference between the results for the different values of m is always bigger between *m*=2 and *m*=3 than between *m*=3 and *m*=4, which implies that, as this parameter increases, there is less dependence of results on it.


### *ACKNOWLEDGEMENTS*

The authors wish to acknowledge the financial support provided by the Spanish Institutions: MCYT (Grant MAT2002-01831), MEC (Grant BIA2005-08965), MICINN (Grant BIA2008-06810 and BIA2011-27870) and JCyL (Grants SA067A05, SA111A07 and SA039A08).


## REFERENCES


1. Levan, A., Royer, J. (1993) *Int. J. Fract.* **61**, 71-99.
2. Carpinteri, A. (1993) *Int. J. Fatigue* **15**, 21-26.
3. Couroneau, N., Royer, J. (1998) *Int. J. Fatigue* **20**, 711-718.
4. Shin, C.S., Cai, C.Q. (2007) *Int. J. Fatigue* **29**, 397-405.
5. Lin, X.B., Smith, R.A. (1997) *Int. J. Fatigue* **19**, 461-469.
6. Lin, X.B., Smith, R.A. (1998) *Int. J. Mech. Sci.* **40**, 405-419.
7. Shih, Y.-S., Chen, J.-J. (1997) *Int. J. Fatigue* **19**, 477-485.
8. Astiz, M.A. (1986) *Int. J. Fract.* **31**, 105-124.
9. Couroneau, N., Royer, J. (2000) *Comput. Struct.* **77**, 381-389.
10. Da Fonte, M., de Freitas, M. (1999) *Int. J. Fatigue* **21**, 457-463.
11. Shih, Y.-S., Chen, J.-J. (2002) *Nucl. Eng. Des.* **214**, 137-145.
12. Shin, C.S., Cai, C.Q. (2004) *Int. J. Fract*. **129**, 239-264.
13. Toribio, J., Matos, J.C., González, B., Escuadra, J. (2009) *Struct. Durab. Health Monit.* **123**, 1-16.
14. Paris, P.C., Erdogan, F. (1963) *J. Basic Eng.* **85D**, 528-534.
15. Toribio, J., Matos, J.C., González, B., Escuadra, J. (2009) *Eng. Fail. Anal.* **16**, 618-630.